ELSEVIER

Powder Technology 121 (2001) 205–212

POWDER TECHNOLOGY

www.elsevier.com/locate/powtec

A transient method for determination of saturation carrying capacity

Esmail R. Monazam [a], Lawrence J. Shadle [b,*], Larry O. Lawson [b]

[a] *REM Engineering Services, 3566 Collins Ferry Rd., Morgantown, WV 26505, USA*

[b] *National Energy Technology Laboratory, U.S. Department of Energy, M / S N04, P.O. Box 880, Morgantown, WV 26507-0880, USA*

Received 16 November 2000; received in revised form 16 February 2001; accepted 27 March 2001

Abstract

Clear definition of smooth and stable operating regimes is necessary if circulating fluid bed reactors are going to be adopted commercially for process applications that require load following capabilities. One significant source of instability or long-term transient occurs when traversing the transition from transporting in a lean phase fluidization regime to transporting in a turbulent or fast-fluidized bed regime. The gas saturation carrying capacity (SCC) is the key functional parameter required to define this transition. A simple method is presented to accurately determine the SCC in which the solids flux was abruptly halted and the loss in pressure signal monitored over time. The SCC was measured for PVC under a variety of conditions. Upon drawing from the analogous liquid–vapor to vapor phase transition, a predictive relationship is also presented to estimate SCC for various gas–solid flow systems, knowing the gas velocity and solids' terminal velocity in that gas. Published by Elsevier Science B.V.

Keywords: Circulating fluid bed; Saturation carrying capacity; Gas–solids flow; Transport regimes

1. Introduction

Circulating fluidized beds (CFBs) are utilized in many different applications, including combustion and gasification of coal. In the design of the riser section of the CFB, the main consideration is generally that of choosing the correct gas velocity at which to transport the solids. Too low a velocity will result in unacceptable, unstable slugging flow; too high a velocity will result in excessive gas requirements, erosion, attrition and high pressure drop. Over the years, there have been number of different and controversial studies exploring the operating regimes of CFB. According to the two-phase theory of fluidization [1–4], when the gas velocity exceed minimum fluidization velocity (U_{mf}), gas bubbles may appear throughout the bed. When the gas velocity exceeds a certain value, turbulent fluidization occurs which is accompanied by high particle carryover rates. At gas velocities greater than those for turbulent fluidization, the solids are carried out of the bed so rapidly that they are considered to be in the transport regime.

The most dilute transport regime is the homogenous dilute transport regime (I). This is characterized as a uniform void fraction both along the vertical and horizontal axes of the riser (Fig. 1). As the solids flux is increased, the void fraction increases uniformly along the length of the riser; however, the radial distribution of solids becomes non-uniform. The solids tend to fall in denser clusters along the wall and rise in a more dilute concentrations towards the center, producing a core-annular flow (II). These regimes (I and II) represent lean phase fluidization and are characterized as fluid-dominating (FD). The onset of fast fluidization (III) is observed when, at a given gas velocity, the solids flux is increased to the point where a dense-phase transport region forms in the lower regions below a dilute-phase transport region in the upper part of the riser. The fully developed fast-fluidized bed regime (III) exhibits a gradual transition between the lower dense bed and the upper dilute bed that has been described as either an S-shape profile [1] or a simple exponential profile in solid concentration along the length of the riser [2]. This regime is characterized as particle-fluid compromising (PFC). The void fraction of the dense bed depends on the gas velocity (in addition to the gas and solids properties) while the void fraction in the upper dilute region also depends on the solids flux. As long as the solids flow rate is below the solids carrying capacity for a given gas velocity, then the circulating fluid bed remains in lean phase, FD, transport regimes (I and II) [1,3–5].

In the literature, various approaches are taken to determine the saturation carrying capacity (SCC) of gas for

* Corresponding author.

0032-5910/01/$ - see front matter. Published by Elsevier Science B.V.
PII: S0032-5910(01)00354-0

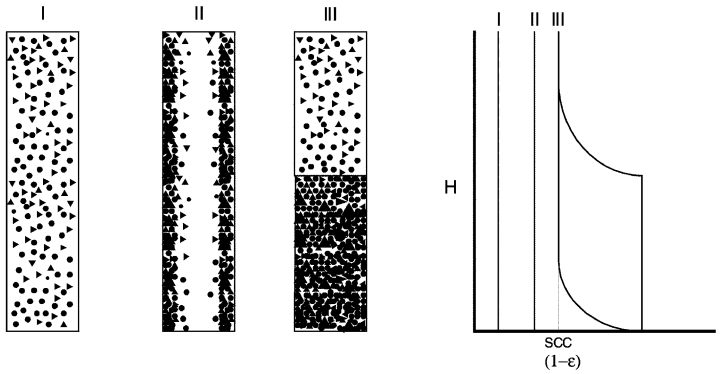

Fig. 1. Schematic of transport fluidization regimes representing fluid-dominated regimes (FD) for dilute (I) and core-annular (II) flow, as well as the particle-fluid compromising regimes (PFC) for fast-fluidization (III). The SCC demarcates the transition between PFC and FD.

gas–solid suspensions. The first approach has defined SCC of gas as the entrainment rate above the transport disengagement height (TDH) where the rate is constant along the freeboard height [6,7]. This approach has proven to estimate the SCC for bubbling and turbulent fluidized bed; however, its extension to the transport regimes has not been demonstrated. In these dilute regimes, the entrainment rate of solids rapidly depletes the inventory of solids in the bed. This adds experimental constraints that necessitate a different data analysis scheme as is presented in this paper.

In the second approach the results from studies on the choking phenomena are interpreted as being related to the SCC. Li [5] describes the solids flow rate, which defines the boundary between the PFC (dilute–dense voidage in riser) and FD (dilute voidage region only) regimes as corresponding to SCC and being synonymous to the choking velocity. Choking velocities and their relationship to changes in fluidization regime are reviewed by Bi et al. [8]. Leung et al. [9] defines choking as the point at which dilute phase flow with constant axial voidage undergoes a sharp transition to a slugging dense phase region. Choking is found to be a function of the gas and solid properties, and the pipe diameter [10]. Several investigators [11–14] have developed mathematical correlations to predict the choking velocity. Bai and Kato [15] noted that choking does not reflect the maximum transport capacity of the flowing gas stream, it just defines a condition in the transport line. The pipe diameter plays a significant role in the choking conditions; therefore, choking appears to contradict the physical interpretation of SCC.

According to Li's [5] theoretical analysis, the fast fluidization regime has S-shape voidage profile and whenever the S-shaped profile appears, the corresponding solid flow rate is bound to be equal to the SCC for a given gas velocity. The most commonly used experimental approach [7,15,16] is to increase the solids circulation rate and evaluate the change in voidage over an incremental length along the riser. Bai and Kato [15] determine the SCC of the gas by plotting the solid holdup at the bottom of the riser against the solid circulation rate. The SCC of the gas was identified as the condition in which the solid-holdup achieves saturation independent of solid circulation rate, the geometry of the riser, or the system configuration. Namkung [16] defined the SCC of the gas as when the solid holdup in the upper dilute region exhibits a maximum value and dense bed forms in the bottom region. Bai et al. [17] developed a transient method to measure type A choking by increasing solids flow and determining the change in slope of the solids inventory increasing the riser. However, these methods can be affected by the solids inventory, the rate of ramp in the solids flow, identifying small variations in similar slopes, and the accuracy of the method used to measure the solids flow rate. When measuring the solids circulation rate using a continuous device, we have found that process dynamics in the CFB can permit short-term surges in solids circulation rates that cannot be sustained in a CFB operated with constant inventory [18]. In addition, geometric considerations can affect the response of incremental pressure drops along the riser. The effect of acceleration of solids at the entry and exit of the riser depends on the respective geometry of the solids and gas inlets and outlets. For example, a smooth, long-radius bending elbow at the exit has much less tendency to reflect solids back down into the upper regions of the riser than does a 90° or tee-shaped elbow [19]. In this study, an experimental method is presented to unambiguously measure the SCC for a given solid at a known gas velocity. However, there has been no definitive theory proposed to predict SCC for a given gas velocity.

2. Experiment

The experimental set up used in this work is shown in Fig. 2. It consisted of a riser of 30.48 cm diameter and 21.3 m high and a standpipe of 0.25 m diameter. A solids transfer leg and a cyclone connected both. The solids transfer device was an L-valve that was 1.52 m long and

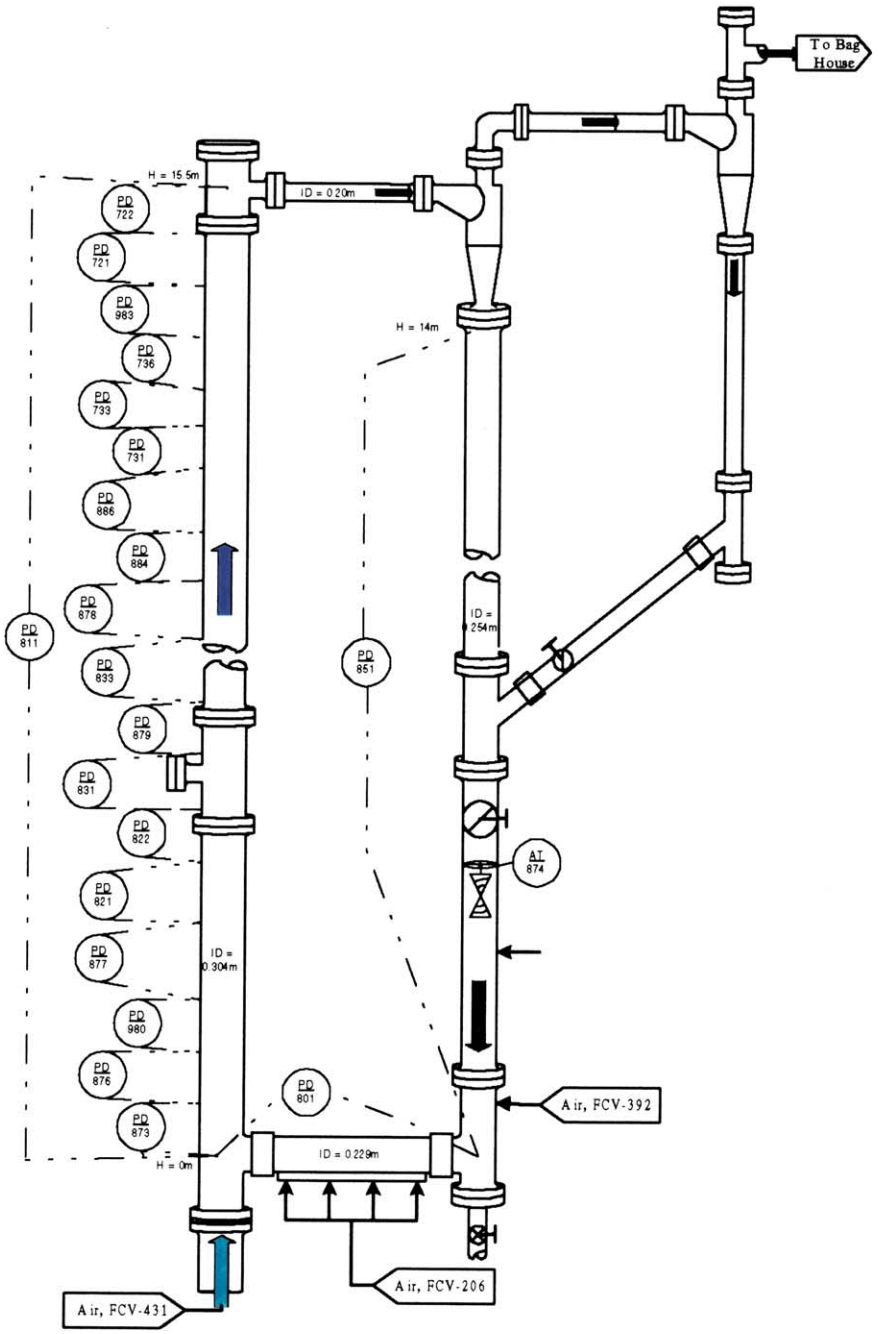

Fig. 2. Schematic of cold flow CFB test facility showing relative locations for key process instrumentation including pressure differentials (PD), flow control valves (FCV), and the analytical transmitter (AT) used for the solids flow rate measurement.

had a 0.23-m diameter. The solids were separated from the gas by two cyclones. The main fluidizing air (FV-431) was fed through a perforated plate into the riser. FV-392 is an aeration port located near the base of the standpipe approximately 0.4 m above the L-valve. It is commonly referred to as the move air because it has been found to directly impact the solids flow rate. A helical-shaped spiral vane was installed in a standpipe (~4 m above the L-valve solids inlet) and the frequency of its revolution was recorded to measure the solids flow rate. The spiral frequency was calibrated for each bed material by draining solids from the bottom of the standpipe over a period of time and weighing the solids. This calibration confirmed that the measurement device yielded volumetric solids velocity data with no slip along the spiral. The solids mass flow was computed continuously for each 10-s interval from this volumetric flow, correcting for the bulk density of different materials.

To minimize static charge buildup, the riser consisted of carbon steel segments except for one 1.22-m acrylic sec-

tion at the base. It was equipped with 23 differential pressure transmitters that were connected in series to measure the incremental pressure drops along the bed. Pressure balance around the CFB loop was checked comparing the sum of the standpipe incremental pressure gains with that from the riser pressure drops. In addition, the sum of the incremental pressure drops across the riser was routinely verified against an overall riser pressure drop measurement. All continuous data for a given steady-state operating condition was time-averaged over a 5-min period.

3. Experimental procedure

During an experiment, the air velocity in the riser was controlled at a constant level and the solid circulation rate was increased by adjusting the move air (FV-392) until exceeding the SCC of the gas. The SCC of the gas is defined based on the voidage profile along the riser. If the voidage profile has the S-shape with the co-existence of two regions (dense at the bottom of the riser and dilute at the top), then the solid circulation rate has reached the SCC. The voidage profiles were determined from the incremental pressure gradient measurements along the riser assuming negligible contribution of acceleration and wall friction.

The measurement of the SCC was obtained in two ways. In the first method, following the commonly reported approach, the riser flow was established without solids flow; it was empty. Aeration was introduced into the L-valve and upper standpipe at a constant rate. Then ramping the move air increased the solids circulation rate. By observing the trend of pressure drops across the riser and comparing to that of solids circulation rate, a point of deviation from FD (dilute) to PFC (dense–dilute regime) could be determined. When the riser reached the PFC regime, the increase in move air produced increasing pressure drop across the riser, but the solids circulation rate stopped increasing (Fig. 3). In this method the SCC is defined as the solids flow rate marking this transition.

In our new method, the riser is brought to a steady-state condition within the PFC regime, perhaps by the same sequence described above, and the solids circulation rate is abruptly stopped. This was accomplished by diverting the flows being introduced into the L-valve and standpipe (including the move air) to the atmosphere. As the solids inventory was being carried from the riser, the pressure drop across the riser decreased. The pressure drops across the riser were recorded as a function of time at a sampling rate of 1 Hz.

In these tests, the bed material used was polyvinyl chloride (PVC). The material properties are presented in Table 1. In order to avoid interference due to static charge, the air relative humidity was maintained above about 40% by introducing steam when necessary.

Table 1
Polyvinyl chloride (PVC) properties

ρ_s (g/cm^3)	1.42
ρ_b (g/cm^3)	0.54
d_p (μm)	180
U_{mf} (m/s)	0.013
U_t (m/s)[a]	0.98

[a] Calculated from ERGUN equation assuming the limit where the void fraction = 1.

4. Results and discussion

The axial pressure profiles along the riser of CFB are displayed in Fig. 4 for different superficial gas velocities. These measurements are conveniently used to infer axial voidage profile by assuming that the only contribution to the axial pressure drop is hydrostatic head of solids (i.e. negligible contribution of acceleration and wall friction).

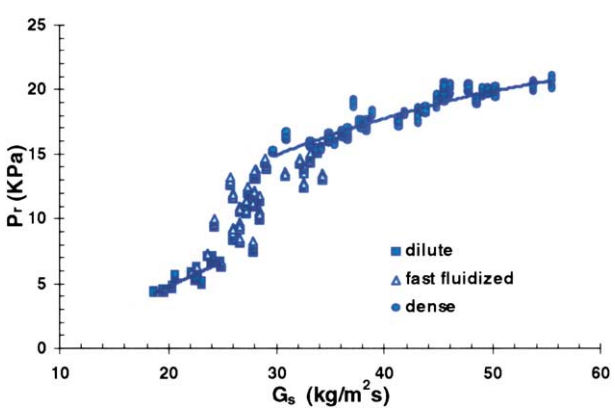

Fig. 3. Riser pressure differential as a function of the solids circulation rate that was varied using a move air ramp of 4.7 slpm/min from about 30 to 120 slpm for PVC that was transported using U_g = 6.35 m/s under mass flow control.

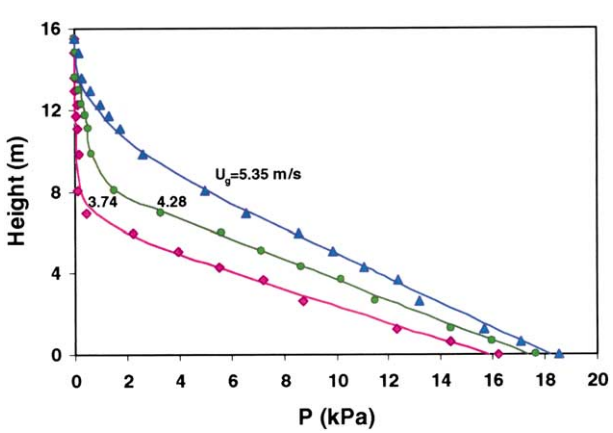

Fig. 4. Pressure profile along the height of the riser for PVC transported using different gas velocities (3.74, 4.28, and 5.35 m/s) under mass flow control.

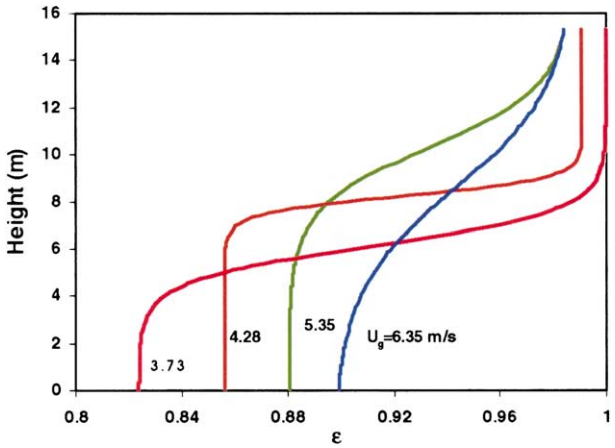

Fig. 5. Voidage profiles along the height of the riser for PVC using different gas velocities (3.74, 4.28, 5.35, and 6.35 m/s) under mass flow control.

The axial voidage may be related to the pressure drop through the following expression [20]:

$$\frac{dP}{dz} \approx \rho_s(1-\varepsilon)g \tag{1}$$

Li and Kwauk [1] proposed an equation for axial voidage profile for fast fluidized bed as:

$$\frac{\varepsilon-\varepsilon_a}{\varepsilon^*-\varepsilon} = e^{(z-z_i)/z_o} \tag{2}$$

substituting Eq. (2) into Eq. (1) and integrating [20]:

$$P(z) = \rho_s g z_o\left[(\varepsilon_a-1)\frac{z_i-H+z}{z_o} - (\varepsilon_a-\varepsilon^*)\ln\left[1+e^{\left(\frac{zi-H+z}{zo}\right)}\right]\right] + \text{const} \tag{3}$$

The parameter z_i is the location of the inflection point of the voidage profile and z_o represents the length of the transition region between the dilute and dense regions. When z_o approaches 0, a clear interface between the dense and dilute regions is indicated, but when z_o approaches infinity it implies a uniform axial profile of the voidage. The parameters ε_a and ε^* are asymptotic voidages characteristic of the voidage profile, where ε_a represents the dense voidage at the bottom of the riser and ε^* the dilute voidage at the top. The H is the riser height, and z is the vertical coordinate. The values of ε_a, ε^*, z_i, z_o, and the integration constant were obtained by curve fitting the axial pressure drop measurements with the expression in Eq. (3) using TABLECURVE available from SPSS. The fit of Eq. (3) to the axial pressure drop measurements is illustrated in Fig. 4 for several different riser velocities. Agreement is very good over the entire riser length with overall variance explained greater than 99%. This estimated voidage profile produced pressure drops equivalent to the measured values when substituted back into Eq. (2).

The calculated axial voidage profile along the riser is presented in Fig. 5 for different riser gas velocities. The voidage profiles clearly provide evidence that there is an interface between dense and dilute-phase regions. These profiles also indicates the appearance of an S-shaped voidage profile that is characteristic of the fast fluidization regime.

Table 2 is a summary of the test case data including the estimated SCC. These tests include various gas velocities all of which were operated in an S-shaped voidage profile in the riser immediately prior to solids flow cut-off. The overall pressure drops, voidage profiles, and height of the interface between dense and dilute bed are characteristic of a CFB operated with constant solids inventory.

According to Li [5], a CFB operating in the fast fluidized regime can be characterized in the following manner. The riser exhibits an S-shaped voidage profile. Variations in the solids inventory in the riser does not result in any change of mass circulation rate, ε_a, and ε^*, but only displaces the position of the inflection point z_i. In other words, the solids flow rate is always equal to the saturation solids carrying capacity at the corresponding gas velocity. In addition, the two asymptotic voidages, ε_a (dilute region), and ε^* (dense region), are only a function of the gas velocity and relevant material properties when in the fast fluidized regime. If the solids control valve is fully closed when in this regime, then the local state of each regime (dilute and dense) will not be changed; however, the top dilute region will extend toward the bottom with a constant solid flow rate (equal to the SCC) until the dense region disappears. Beyond this point in time the bed empties.

The pressure gradient across the riser is displayed in Fig. 6 as a function of time without circulating or feeding any fresh solids. As expected, an increase in the gas velocity decreases the time required to empty the bed. These measurements are used to predict the SCC for the corresponding gas velocity. The data points in Fig. 6

Table 2
Summary of the test case data

U_g (m/s)	G_s^* (kg/m^2 s)	ε_a	ε^*	z_o (m)	z_i (m)	ε_{avg}
3.22	2.5	0.824	0.999	0.74	6.1	0.93
3.74	3.8	0.839	0.998	0.76	5.8	0.94
4.28	7.8	0.856	0.99	0.37	8.2	0.92
4.78	11.4	0.873	0.977	0.48	8.4	0.92
5.30	13.8	0.880	0.980	1.30	10.4	0.91
5.85	19.4	0.894	0.954	0.20	8.0	0.92
6.35	20.5	0.902	0.962	0.20	9.6	0.92
6.90	28.1	0.905	0.945	0.03	7.0	0.93

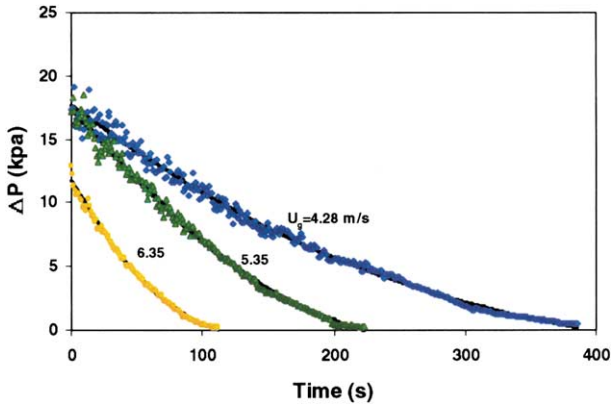

Fig. 6. Decay profiles for overall riser pressure drop (PD-811) for PVC after halting solids flow but while maintaining different gas velocities (4.28, 5.35, and 6.35 m/s) under mass flow control. Test data are represented as symbols while the lines represent the least squares fit to Eq. (8).

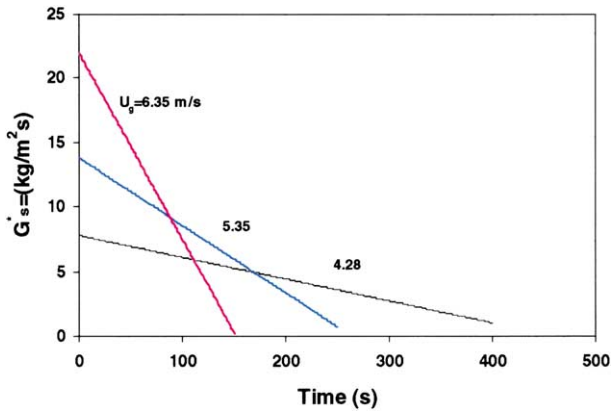

Fig. 7. Estimates for PVC solids flux exiting the riser as a function of time after the solids flow as halted.

represent the measured pressure drop across the overall riser while the line is the fit to the following analysis.

Under transient operation (during the emptying time), the solids material balance can be written as:

$$\frac{1}{A}\frac{\mathrm{d}m}{\mathrm{d}t} = -G_{s,o} \tag{4}$$

where m is the solids inventory in the riser, A is the riser cross-sectional area, and $G_{s,o}$ is the solids flux leaving the riser at any time t.

Assuming that the mass inventory inside the riser as a function of time is proportional to the pressure gradient across the riser, then one can obtain Eq. (5).

$$m(t) = p(t)^{*} A/g \tag{5}$$

Differentiating Eq. (5) with respect to time results in Eq. (6):

$$\frac{\mathrm{d}m(t)}{\mathrm{d}t} = \frac{A}{g}\frac{\mathrm{d}p}{\mathrm{d}t} \tag{6}$$

Substituting Eq. (6) into Eq. (4) produces the flux as a function of the rate of pressure drop:

$$G_{s,o} = -\frac{1}{g}\frac{\mathrm{d}p}{\mathrm{d}t} \tag{7}$$

During the emptying process, the pressure gradient across the riser was measured as a function of time (Fig. 6). To evaluate the solids flux during the emptying time using Eq. (7), one must differentiate the data either numerically or graphically. We chose to determine $\mathrm{d}p/\mathrm{d}t$ by numerical differentiation. The pressure drop across the riser was fitted to the following simple equation:

$$\Delta p^{0.5} = a + bt \tag{8}$$

The plot of Δp vs. time for different gas velocity and the corresponding Eq. (8) fit is shown in Fig. 6. Agreement is very good over the entire emptying time with variance explained $> 99.9\%$. Solids flux was obtained at various times during the emptying process by differentiating Eq. (8) and substituting into Eq. (7). The solids flux leaving the riser during the emptying process is presented in Fig. 7 for different gas velocities that were operating in the fast fluidized regime. SCC for the PVC bed material was determined for each corresponding gas velocity as the solids flux at the emptying time = 0. Thus, in the fast fluidized regime or higher (solids loading), the solids flux extrapolated to $t = 0$ represents the SCC, G_s^*.

The solids fluxes and riser pressure drops were also measured for a series of operating conditions in the steady-state time period immediately prior to conducting the solids flow cut-off experiments (Table 3). The solids flux measurements, G_s, were consistently higher than the SCC—those fluxes (at $t = 0$) estimated from the solids cut-off experiments, G_s^* (Fig. 8). The difference between these two values was reduced as the measured steady-state solids flux approached the SCC. This is demonstrated in

Table 3
Summary of the test case data

U_g (m/s)	Δp (kPa)	G_s^* (kg/m^2 s)	$G_s \pm$ std. dev. (kg/m^2 s)
3.22	15.34	2.5	3.2 ± 1.1
3.74	13.27	3.8	5.5 ± 1.3
4.28	17.37	7.8	13.0 ± 1.4
4.78	17.64	11.4	22.0 ± 2.8
5.30	17.11	13.8	25.5 ± 2.0
5.85	14.82	19.4	42.8 ± 4.4
6.35	16.78	22.0	52.0 ± 9.7
6.35	14.58	20.5	35.0 ± 2.4
6.35	12.84	18.9	26.9 ± 1.8
6.35	10.78	19.6	24.8 ± 1.5
6.90	12.92	28.1	60.0 ± 3.6

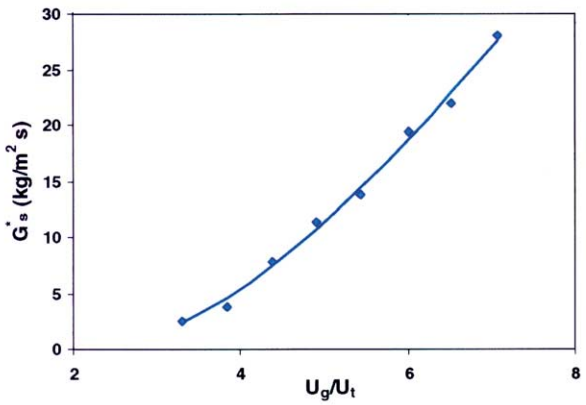

Fig. 8. The SCC as a function of gas velocities relative to solids terminal velocity. SCC was determined from a solids (PVC) decay curve after halting the solids circulation rate while in the PFC regime by extrapolating the solids flux exiting the riser to $t = 0$.

the series of test points collected at 6.35 m/s riser velocity, varying only the move aeration. For these constant velocity cases, the SCC solids fluxes, G_s^*, obtained using the cutoff method were equivalent (± 1.3 kg/m^2 s) within experimental variability (average standard deviation of ± 3.9 kg/m^2 s). Moreover, the replicate measurements of G_s^* agreed within the time-dependent variability of the measured solids flux, G_s, for even the most stable condition (± 1.5 kg/m^2 s). However the steady-state solids fluxes measured varied dramatically by more than a factor of two.

The steady-state fluxes measured prior to the cut-off were obviously not equivalent to the SCC. When operating in a fast fluidized or PFC regime, the continuous solids flux measurement takes on some characteristics of the dense transport regime. In other words, the continuous process measurement, G_s, was higher than the solids cutoff measurement of the SCC due to flow-out of the more dense riser bed when in PFC. This leads to the conclusion that an SCC measurement using the steady-state method can be biased high.

According to Zenz and Othmer [21] the gas/solid systems may be usefully considered as a two-phase system analogous to the phases of vapor–liquid. Although the transport of solid particles by a gas stream exhibits some behavior not usually seen in vapor–liquid, there are many similarities [22]. The onset of a transition from a dilute phase at a particular value of gas velocity to a dense phase, and the instability of this phase separation in the vicinity of onset, suggested to us a useful correspondent with vapor–liquid systems. These similarities have led a number of authors to postulate several phase-diagram approaches. The similarity between the Matsen [11] phase diagram and the PVT surface of an vapor–liquid system led Klinzing et al. [22] to suggest a one-to-one correspondence, respectively, between the solids flux, gas flux, and the reciprocal solids volume fraction in a gas/solid systems with the pressure, temperature, and volume in a vapor/liquid system. Therefore, the SCC is correlated similar to the Clapeyron equation as:

$$G_s^* = \exp\left(5.485 - \frac{16.48}{U_g/U_t} + \frac{0.9989}{(U_g/U_t)^2}\right) \quad (9)$$

where U_g and U_t are superficial gas velocity and terminal velocity in m/s. On the basis that this thermodynamic analogy is valid, Eq. (9) represents an attempt to provide a predictive relationship for the SCC given only the gas and solids properties (U_t) and the gas velocity (U_g).

This relationship (Eq. (9)) is expected to be valid, at its lower limit, for the gas velocities approaching the terminal velocity. At high velocities the equation is constrained by the transport velocity. However, unambiguous measurement of the transport velocity is not yet well-defined. In the vapor–liquid analogy, the upper limit is the critical temperature where liquid, vapor and steam coexist. In fluidization, the upper transition is difficult to identify at higher flows because the dense bed voidage approaches that of the dilute bed region and the transition becomes hard to distinguish. While this transition is easier to identify at low flows, it is more difficult to measure due to the difficulty of maintaining sufficient solids inventory in a CFB system to generate dense bed voidages in the volume available in the riser.

Bi and Fan [14] and Bai and Kato [15 have proposed correlations to determine the SCC of the gas for various materials. A comparison between our data and their correlations is illustrated in Fig. 9. The data displayed the same type of vessel diameter dependence reported by Xu et al. [23]. The G_s^* data reported here from a 0.3-m diameter vessel was lowest, 0.15 m was intermediate [14], and the

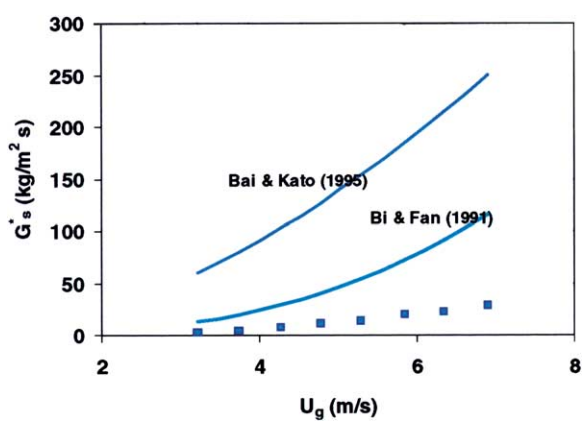

Fig. 9. Comparison of the correlation to estimate the SCC for PVC from test data (symbols) with literature estimates (lines) taken from Bi and Fan [14] and Bai and Kato [15]. Riser diameter is equal to 0.3, 0.15, and 0.1 m, respectively.

smallest vessel of 0.1 m was the highest [15]. Converting the SCC to a mass flow rate, however, eliminates this systematic variation and produces quite good agreement between all three correlations independent of vessel size. More investigation of this observation is needed. On this basis, the literature correlations agree reasonably well with the correlation developed from the liquid–vapor phase analogy.

5. Conclusion

A new method has been presented for determining an unambiguous SCC for a gas–solid flow system. The method is based on transient pressure drop measurement across the riser during a solids flow cut-off experiment while maintaining constant gas flow. When the first derivative with respect to time is extrapolated back to the time that solids flow was halted, a solids flux can be determined. This solids flux is equivalent to the SCC for that gas velocity when the initial state of the bed is PFC (fast fluidized or denser). This method for estimating SCC avoids the inaccuracies associated with measuring circulation rates. Also this method does not rely on measurements of pressure drops as taken during conditions that display significant hysteresis because of their proximity to flow regime transition. Furthermore, this method does not depend upon measuring small variations in similar time-dependent slopes as is the case for other transient methods reported.

The method reported here is inherently accurate. When the solids flow is cut-off from a densely loaded bed, a measurement of the rate of solids leaving the bed is a direct measurement of the solids elutriation rate and thus the SCC. Analysis of this type of transient data may also permit researchers to estimate the steady-state solids flux for lean phase fluidization regimes.

Symbols

A	riser cross-sectional area (m^2)
d_p	particle size (μm)
g	acceleration due to gravity (m^2/s)
G_s	solids flux (kg/m^2 s)
$G_{s,o}$	solids flux leaving the riser (kg/m^2 s)
G_s^*	solids flux at SCC (kg/m^2 s)
H	riser height (m)
P	pressure (kPa)
m	mass inventory inside the riser (kg)
t	time (s)
U_g	superficial gas velocity (m/s)
U_{mf}	minimum fluidization velocity (m/s)
U_t	particle terminal velocity (m/s)
z	vertical coordinate (m)
z_i	location of the inflection point (m)
z_o	characteristic length (m)

Greek letters

ε	voidage
ε_{avg}	integrated average voidage
ε_a	limiting voidage of the dense phase
ε^*	limiting voidage of the dilute phase
ρ_s	solid density (g/cm^3)
ρ_b	bed density (g/cm^3)
Δp	pressure drop across the riser (kPa)

Acknowledgements

The authors acknowledge the Department of Energy for funding the research through the Fossil Energy's Integrated Gasification Combined Cycle program. Operations of the CFB unit was made possible with support from Jim Devault and Todd Worstell.

References

[1] Y. Li, M. Kwauk, in: J.R. Grace, J.M. Matsen (Eds.), Fluidization. Plenum, New York, 1980, p. 537.
[2] D. Kunii, O. Levenspiel, Powder Technol. 61 (1990) 193.
[3] C.S. Teo, L.S. Leung, in: N.P. Cheremisinoff (Ed.), Encyclopedia of Fluid Mechanics. Solids and Gas–Solids Flows, vol. 4, Gulf Publishing, Houston, 1986, pp. 611–663.
[4] L.-S. Fan, C. Zhu, Principles of Gas–Solids Flows. Cambridge University Press, 1998, pp. 421–460.
[5] J. Li, Modeling. in: M. Kwauk (Ed.), Fast Fluidization. Academic Press, 1994, p. 147.
[6] F.A. Zenz, N.A. Weil, AIChE J. 4 (1958) 472.
[7] C.Y. Wen, L.H. Chen, AIChE J. 28 (1982) 117.
[8] H.T. Bi, J.R. Grace, J.-X. Zhu, Int. J. Multiphase Flow 19 (1993) 1077.
[9] L.S. Leung, in: J.R. Grace, J.M. Matsen (Eds.), Fluidization. Plenum, New York, 1980, p. 25.
[10] L.S. Leung, Pneumotransport 5, London, A 3 (1980) 35.
[11] J.M. Matsen, Powder Technol. 32 (1982) 21.
[12] Y. Yousif, G. Gau, Chem. Eng. Sci. 29 (1974) 1939.
[13] W.C. Yang, Powder Technol. 35 (1983) 143.
[14] H.T. Bi, L.S. Fan, AIChE Anuual Meeting, Los Angeles, November. 1991, p. 17.
[15] D. Bai, K. Kato, J. Chem. Eng. Jpn. 28 (1995) 179.
[16] W. Namkung, S.W. Kim, S.D. Kim, Chem. Eng. J. 72 (1999) 245.
[17] D. Bai, A.S. Issangya, J.R. Grace, Powder Technol. 97 (1998) 59.
[18] L.O. Lawson, L.J. Shadle, Proceedings of the 15th International Conference on Fluidized Bed Combustion, FBC99-0117. 1999, p. 21.
[19] Y. Li, Modeling. in: M. Kwauk (Ed.), Fast Fluidization. Academic Press, 1994, p. 136.
[20] M. Louge, H. Chang, Powder Technol. 60 (1990) 197.
[21] F.A. Zenz, D.F. Othmer, Fluidization and Fluid-Particle Systems. Reihold Chemical Eng. Series, Reinhold Publishing, New York, 1960.
[22] G.E. Klinzing, N.D. Rohatgi, A. Zaltash, C.A. Myler, Powder Technol. 51 (1987) 135.
[23] G. Xu, K. Nomula, N. Nakagawa, K. Kato, Powder Technol. 113 (2000) 80.